MIB-1 index of 1% in Case 5. No correlation between size and tumor fluorescence was observed.

Representative cases

Case 3: A 37-year-old woman presented with headache and mild right hemiparesis. MR imaging showed a large meningioma (maximum diameter 59 mm) at the left parasagittal area, extending to the skull and causing the skull to bulge (Figure 1A). After craniotomy, it was found that the meningioma invaded into the inner layer of the skull and fluoresced charcoal-red (Figure 1B). The invasion of meningioma into the inner layer was drilled out until the charcoal-red light disappeared, and the skull was returned at closure. The parasagittal meningioma fluoresced strongly and was removed totally, and the attachment to the lateral wall of the superior sagittal sinus was coagulated (Figures 1C and 1D). The patient had no neurological deficit at discharge. The histopathological diagnosis was transitional meningioma with a MIB-1 index of 2%.

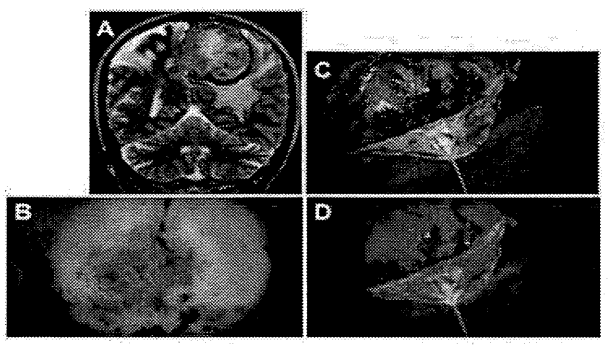

Figure 1: Case 3 of a 37-year-old woman with parasagittal meningioma. A: Preoperative T2-weighted MR image showing the large tumor with peritumoral edema that reached the superior sagittal sinus. B: Intraoperative photograph in the fluorescence mode of skull from intracranial side showing skull invasion of the tumor. C and D: Intraoperative photograph in the white-light mode of the surface of the main tumor mass after opening the dura mater (C), and the main tumor mass showed bright fluorescence in the fluorescence mode (D).

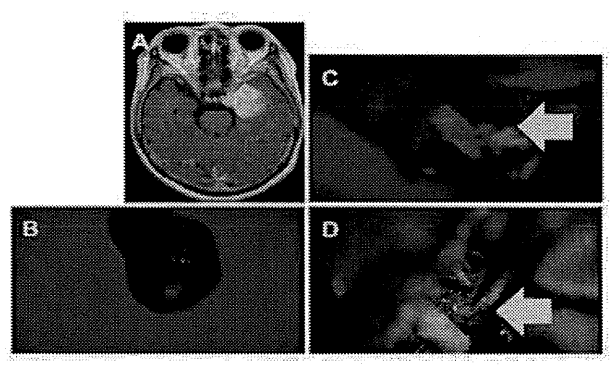

Figure 2: Case 4 of a 67-year-old woman with left sphenoid ridge meningioma. A: Preoperative gadolinium-enhanced T1-weighted MR image showing the main tumor with peritumoral edema. B: Intraoperative photograph in the fluorescence mode of the resected tumor showing some fluorescences. C and D: Intraoperative photograph in fluorescence mode of the tumor encased the left middle cerebral artery and invaded into the brain parenchyma showing fluorescence.

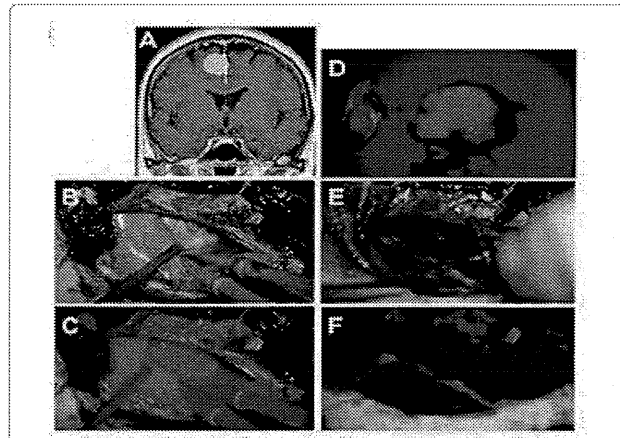

Figure 3: Case 10 of a 59-year-old woman of a right falx meningioma. A: Preoperative gadolinium-enhanced T1-weighted MR image showing the main tumor of right falx. B and C: Intraoperative photograph in fluorescence mode of the tumor showing bright fluorescence. D: The resected tumor (right) and the opposite side of the attachment of the resected falx (left) showed bright fluorescence. E and F: Intraoperative photograph in fluorescence mode of the falx coagulated showing no fluorescence.

Case 4: A 67-year-old woman presented with diplopia and headache. MR imaging showed a left sphenoid ridge meningioma with intratumoral hemorrhage and parenchymal edema adjacent to the tumor (maximum diameter 44 mm) (Figure 2A). The tumor encased the left middle cerebral artery and invaded into the brain parenchyma with charcoal-red fluorescence (Figures 2B and 2D). The tumor was resected totally until no fluorescence was observed. The patient had no neurological deficit and no epileptic seizures after operation. The histopathological diagnosis was meningothelial meningioma with a MIB-1 index of 2%.

Case 10: A 59-year-old woman presented with headache and mild weakness of the right lower extremity. MR imaging showed a right falx meningioma (maximum diameter 30 mm) (Figure 3A). The tumor showed strong charcoal-red fluorescence (Figure 3B-D). The falx attached to the tumor was coagulated, and the fluorescence disappeared (Figures 3E and 3F). After the attached falx was resected, the resected tumor and the opposite side of the falx to which the tumor was attached showed strong charcoal-red fluorescence (Figure 3D), showing that the meningioma invaded through the falx. The headache and weakness of the lower extremity disappeared after total resection. The histopathological diagnosis was transitional meningioma with a MIB-1 index of 2%.

Discussion

In this study, 5-ALA administration resulted in bright and diffuse tumor fluorescence in 15 (88%) of 17 cases, including the cases in which pre-operative embolization had been performed (Table 1). Protoporphyrin IX (PPIX) fluorescence was seen only in the main mass and areas of tumor invasion. In this series, the sensitivity and specificity of PPIX fluorescence of the main tumor mass were 88% (15 of 17 cases) and 100% (17 of 17 cases), respectively (Table 1). Fluorescence guidance allowed us to identify the extent of the tumor and helped us avoid leaving residual tumor tissue that was difficult to identify in the white-light mode. If we had not used fluorescence guidance, we might not have noticed several small areas of residual tumor showing 5-ALA fluorescence under violet-blue light with an operative microscope in

the operating room. In this study, numerous factors affected tumor recurrence: the tumor's soft consistency, lobular shape, encasement of the artery, invasion into the brain parenchyma, and dural attachment very close to the venous sinus, as well as bone invasion. Because of these factors, the risk of recurrence was considered very high [4-7]. It is worth noting that tumor remnants were identified by fluorescence in multiple regions. deVries and Wakhloo [8] reported that recurrent tumor is often found at multiple sites. Meningioma has a high risk of recurrence, and during excision, meningioma tissue can be left at any attachment to surrounding tissues, especially at attachments to the gliotic brain, major sinuses, the anterior visual pathway [9], and marginal dura mater. Aggressive excision of the dura and gliotic brain has been recommended to reduce this risk [7,10], but the optimal extent of dural resection has been controversial. Kinjyo et al. proposed a margin of 2 cm. Nakasu et al. reported that a 1-cm dural margin is insufficient to prevent recurrence [11,7]. The most suitable margin for dural excision will necessarily differ from case to case, because of differences in tumor growth rates and invasiveness. In light of these factors, photodynamic diagnosis may become a promising method of determining the extent of dural resection.

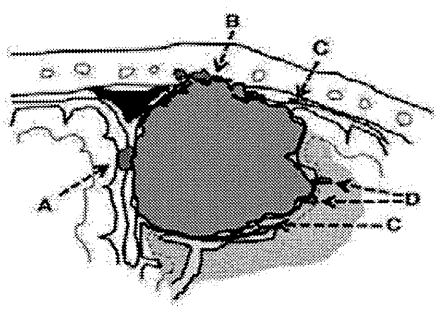

Figure 4: Schematic drawing showing areas most likely to harbor tumor remnants. A: Intradural invasion. B: Bone invasion. C: Dural extension. D: Tumor tissue behind vessels in the sulcus or parenchymal invasion. The gray zone shows the extent of the tumor. The texture close to the tumor shows the extent of brain edema.

On the other hand, indiscriminate excision can lead to complications related to brain and vascular injury. Therefore, if a tumor is located close to a major sinus, the skull base, or an eloquent area, then the excision of dura mater and brain tissue should be restricted to safe areas, and unresectable dura must be coagulated. Fluorescence guidance may help avoid unnecessary excision. The reasons why tumor remnants may be overlooked can be classified into three categories. 1) The tumor cells invade surrounding tissue, attached dura mater, bone, and brain, after which the invaded area is difficult to distinguish from the noninvaded area (Figure 4). 2) The tumor remnants may be hidden behind large vessels or the sinus, dural fold, or sulcus (Figure 4). 3) Daughter lesions may develop apart from the main mass. All three reasons can make tumor remnants difficult to identify with the naked eye or with the aid of a surgical microscope. The use of 5-ALA-induced fluorescence can help surgeons identify tumor remnants, because an area of strong red fluorescence will appear if even a small part of a remnant is present at the tissue surface. Fluorescence can make it easy to distinguish the one from the other and determine the extent of a given tumor.

In the present study, tumor invasion into the skull was also visualized by charcoal-red fluorescence. In most cases, hyperostosis in association with meningioma is related to tumor invasion. However, the extent of tumor invasion is difficult to judge from the appearance alone. Although it is relatively easy to treat bone invasion in cases of convexity meningioma, invasion at the skull base is hard to treat because it involves the cranial nerves, major blood vessels, and air sinuses. Therefore, the detection of bone invasion using photodynamic diagnostic methods would seem to be valuable, especially in surgery for skull-base meningiomas.

Many recent reports have described the usefulness of 5-ALA to identify the margin of a malignant tumor or glioma for maximal cytoreduction [6,12-16]. 5-ALA is an endogenous body metabolite central to heme biosynthesis that is readily absorbed and metabolized into porphyrins by malignant tumor cells (5). This phenomenon can aid in tumor resection to identify the residual tumor in tumor margins, when gross total resection is possible and desirable, with malignant cells fluorescing, allowing discrimination between tumor and normal functional brain tissue [6,12,13]. The side effects of 5-ALA are mild. Skin irritation, nausea, and transient elevation in liver function test

Case No.	Age, Sex	Tumor Location	Tumor Diameter(mm)	Tumor Fluorescence	Preoperative Embolization
1	62, F	rt PO parasagittal	44x40x46	Strong	No
2	62, F	rt F falx	76x49x67	Strong	Yes
3	37, F	lt FP parasagittal	59x58x50	Strong	Yes
4	67, F	lt sphenoid ridge	44x38x40	Weak	No
5	45, F	lt petroclival	28x14x24	Weak	No
6	65, M	rt P convexity	25x19x26	Strong	No
7	75, F	rt sphenoid ridge	21x21x20	Strong	No
8	65, F	lt sphenoid ridge	63x46x59	Strong	Yes
9	74, F	lt P convexity	40x40x46	Strong	No
10	59, F	rt P falx	30x25x21	Strong	Yes
11	75, F	planum sphenoidale	37x33x31	Strong	No
12	81, F	lt F convexity	41x29x28	Strong	No
13	60, F	rt petroclival	26x24x27	Strong	No
14	48, F	planum sphenoidale	22x19x20	Strong	No
15	60, F	rt F convexity	26x18x23	Strong	No
16	64, F	rt sphenoid ridge	32x26x26	Strong	No
17	48, F	lt FP parasagittal	42x32x26	Strong	No

Table 1: Characteristics of patients with meningioma. Abbreviations used in this table: M, male; F, female; PO, parieto-occipital; F, frontal; FP, fronto-parietal; P, parietal; rt, right; lt, left.

results have occurred in some adult patients given higher doses of 5-ALA [4,8,17,18]. Apart from transient nausea after dye ingestion, the present patients had no side effects, and their liver function tests were unchanged.

Accumulation in the normal central nervous system is restricted except in the subependymal zone and choroid plexus [18,19]. Many possible mechanisms have been posited to explain the selective accumulation of PPIX in neoplasms: (1) enhanced penetration of 5-ALA through the blood-brain barrier; (2) reduced transporter activity that drains PPIX outside of cells; and (3) reduced activity of ferrochelatase, which converts PPIX to heme [20]. At least one of these factors is probably involved in the strong 5-ALA-derived fluorescence in meningiomas. In general, there is no strict correlation between cell proliferation and PPIX accumulation. In meningiomas, the proliferation rate is relatively low [12].

In conclusion, applying this method to meningiomas that have a high risk of recurrence should be of value not only in ensuring that tumor remnants are not overlooked during resection but also in helping to avoid unnecessarily radical resection and the associated risk of morbidity. To confirm the usefulness of fluorescence-guided surgery for meningioma, further studies on its sensitivity, specificity, and effect on recurrence rates are needed.

Disclaimer

The authors report no conflict of interest concerning the materials or methods used in this study or the findings reported in this paper.

References

1. Samii M, Gerganov VM (2008) Surgery of extra-axial tumors of the cerebral base. Neurosurgery 62: 1153-1166.
2. Kajimoto Y, Kuroiwa T, Miyatake S, Ichioka T, Miyashita M, et al. (2007) Use of 5-aminolevulinic acid in fluorescence-guided resection of meningioma with high risk of recurrence. Case report. J Neurosurg 106: 1070-1074.
3. Moriuchi S, Yamada K, Dehara M, Teramoto Y, Soda T, et al. (2011) Use of 5-aminolevulinic acid for the confirmation of deep-seated brain tumors during stereotactic biopsy. Report of 2 cases. J Neurosurg 115: 278-280.
4. Al-Mefty O, Kadri PA, Pravdenkova S, Sawyer JR, Stangeby C, et al. (2004) Malignant progression in meningioma: documentation of a series and analysis of cytogenetic findings. J Neurosurg 101: 210-218.
5. Jääskeläinen J (1986) Seemingly complete removal of histologically benign intracranial meningioma: late recurrence rate and factors predicting recurrence in 657 patients. A multivariate analysis. Surg Neurol 26: 461-469.
6. Jääskeläinen J, Haltia M, Servo A (1986) Atypical and anaplastic meningiomas: radiology, surgery, radiotherapy, and outcome. Surg Neurol 25: 233-242.
7. Nakasu S, Nakasu Y, Nakajima M, Matsuda M, Handa J (1999) Preoperative identification of meningiomas that are highly likely to recur. J Neurosurg 90: 455-462.
8. de Vries J, Wakhloo AK (1994) Repeated multifocal recurrence of grade I, grade II, and grade III meningiomas: regional multicentricity (primary new growth) or metastases? Surg Neurol 41: 299-305.
9. Stafford SL, Perry A, Suman VJ, Meyer FB, Scheithauer BW, et al. (1998) Primarily resected meningiomas: outcome and prognostic factors in 581 Mayo Clinic patients, 1978 through 1988. Mayo Clin Proc 73: 936-942.
10. Salcman M (1991) Malignant meningiomas, in Al-Mefty O (ed): Meningiomas. New York: Raven Press, 75–86
11. Kinjo T, al-Mefty O, Kanaan I (1993) Grade zero removal of supratentorial convexity meningiomas. Neurosurgery 33: 394-399.
12. Iinuma S, Farshi SS, Ortel B, Hasan T (1994) A mechanistic study of cellular photodestruction with 5-aminolaevulinic acid-induced porphyrin. Br J Cancer 70: 21-28.
13. Kallio M, Sankila R, Hakulinen T, Jääskeläinen J (1992) Factors affecting operative and excess long-term mortality in 935 patients with intracranial meningioma. Neurosurgery 31: 2-12.
14. Morofuji Y, Matsuo T, Hayashi Y, Suyama K, Nagata I (2008) Usefulness of intraoperative photodynamic diagnosis using 5-aminolevulinic acid for meningiomas with cranial invasion: technical case report. Neurosurgery 62: 102-103.
15. Coluccia D, Fandino J, Fujioka M, Cordovi S, Muroi C, et al. (2010) Intraoperative 5-aminolevulinic-acid-induced fluorescence in meningiomas. Acta Neurochir (Wien) 152: 1711-1719.
16. Bekelis K, Valdés PA, Erkmen K, Leblond F, Kim A, et al. (2011) Quantitative and qualitative 5-aminolevulinic acid-induced protoporphyrin IX fluorescence in skull base meningiomas. Neurosurg Focus 30: E8.
17. Borovich B, Doron Y (1986) Recurrence of intracranial meningiomas: the role played by regional multicentricity. J Neurosurg 64: 58-63.
18. Ennis SR, Novotny A, Xiang J, Shakui P, Masada T, et al. (2003) Transport of 5-aminolevulinic acid between blood and brain. Brain Res 959: 226-234.
19. Olivo M, Wilson BC (2004) Mapping ALA-induced PPIX fluorescence in normal brain and brain tumour using confocal fluorescence microscopy. Int J Oncol 25: 37-45.
20. Peng Q, Warloe T, Berg K, Moan J, Kongshaug M, et al. (1997) 5-Aminolevulinic acid-based photodynamic therapy. Clinical research and future challenges. Cancer 79: 2282-2308.

Citation: Moriuchi S, Yamada K, Dehara M, Teramoto Y, Soda T, et al. (2013) Use of 5-Aminolevulinic Acid to Detect Residual Meningioma and Ensure Total Removal while Avoiding Neurological Deficits. J Neurol Neurophysiol 4: 159. doi:10.4172/2155-9562.1000159

Ann Nucl Med (2013) 27:772–780
DOI 10.1007/s12149-013-0747-z

ORIGINAL ARTICLE

Analysis of progression and recurrence of meningioma using ^{11}C-methionine PET

Hidetoshi Ikeda · Naohiro Tsuyuguchi · Noritsugu Kunihiro · Kenichi Ishibashi · Takeo Goto · Kenji Ohata

Received: 31 January 2013 / Accepted: 16 June 2013 / Published online: 26 June 2013

Abstract
Objective The recurrence rate of meningioma after surgery is high, and progression is often observed. The risk factors for recurrence and progression are not clear. We evaluated the risk factors for recurrence and progression in meningioma using ^{11}C-methionine (MET) positron emission tomography (PET).
Methods Thirty-seven patients (mean follow-up, 80 months) with an intracranial meningioma were enrolled. MET PET was performed before treatment between 1995 and 2010, and patients were followed up in an out-patient clinic. Surgery was performed in 33 patients, and a wait-and-see approach was taken in four patients. We evaluated the extent of tumor resection, location, WHO grade, Ki-67 labeling index, and lesion to normal ratio (LN ratio) of MET uptake.
Results Six of the surgical cases had a recurrence, and two of the observation-only patients had tumor progression. A high LN ratio of MET uptake was a significant risk factor for recurrence and progression with univariate analysis. The area under the curve of receiver operating characteristic curve for the LN ratio of MET uptake was 0.754, and the optimal cutoff value was 3.18 (sensitivity 63 %, specificity 79 %). With multivariate analysis, a high LN ratio of MET uptake, non-gross total resection, and a high WHO grade were significant risk factors for progression and recurrence.
Conclusion A high LN ratio of MET uptake was a risk factor for tumor progression and recurrence. The advantage of MET PET is that it is not invasive and can easily be used to evaluate the whole tumor.

Keywords ^{11}C-methionine PET · Meningioma · Riskfactor of recurrence and progression · Multivariable analysis · ROC analysis

H. Ikeda (✉) · N. Tsuyuguchi · N. Kunihiro · K. Ishibashi · T. Goto · K. Ohata
Department of Neurosurgery, Osaka City University Graduate School of Medicine, 1-4-3 Asahi-machi, Abeno-ku, Osaka 545-8585, Japan
e-mail: hide-i@med.osaka-cu.ac.jp

Introduction

Meningioma is the most common primary brain tumor in adults. The frequency of meningioma among all types of brain tumors is 26.4 % in Japan [1] and 34.4 % in the United States. Many histopathological subtypes exist. Most meningiomas are benign, but World Health Organization (WHO) grade II and grade III meningiomas, which exhibit aggressive clinical behavior, are found in 10 % of patients with meningioma. We usually perform surgery for symptomatic cases or cases with large tumors. For small and asymptomatic cases, a wait-and-see approach is taken. However, gross total resection (GTR) is difficult in some surgical cases because of the tumor location and invasion into the brain tissue and the venous sinus. The residual tumor often recurs with malignancy, making the patient's prognosis poor. Meningiomas that are only observed sometimes progress and require surgical resection. In previous papers, the recurrence rate after surgery was high. Even if the tumor is removed completely, the recurrence rate is between 7 and 32 %. After subtotal resection, the recurrence rate is between 19 and 50 % [2–4].

The risk factors for progression and recurrence in meningioma are not clear, and clarification of these factors is important for determining surgical indications and

treatment strategies. We usually use the Ki-67 labeling index (LI) to evaluate the proliferative activity, but surgery is required to obtain a tissue specimen. Surgery is invasive for the patient, and evaluating the risk of recurrence with the Ki-67 LI is controversial because the tissue specimen sometimes does not reflect the whole tumor.

In this study, we evaluated ^{11}C-methionine (MET) uptake of the whole tumor using MET positron emission tomography (PET) to investigate the risk factors for recurrence and progression.

Methods

Patients

From a database of patients who were examined with MET PET, we retrospectively retrieved data for all 73 patients who were diagnosed with intracranial meningioma between 1995 and 2010. These cases were not a consecutive series. We could not examine MET PET results for all meningioma cases because the number of cases that could be examined by MET PET per week in our facilities is limited. Thirty-seven patients fulfilled the inclusion criteria for this study: (1) patients were initially diagnosed with meningioma; (2) MET PET was performed before surgery or observation; (3) patients were followed at Osaka City University Hospital or affiliated hospitals; (4) during the follow-up period, no additional treatment was performed other than the first surgery. Thirty-three patients were excluded because of recurrence after surgery, and three patients dropped out during the follow-up period. Thus, 37 cases (23 females and 14 males) were enrolled in this study (Fig. 1). The mean age of the patients was 54.5 ± 12.9 years. All study participants provided informed consent, and the study design was approved by an ethics review board.

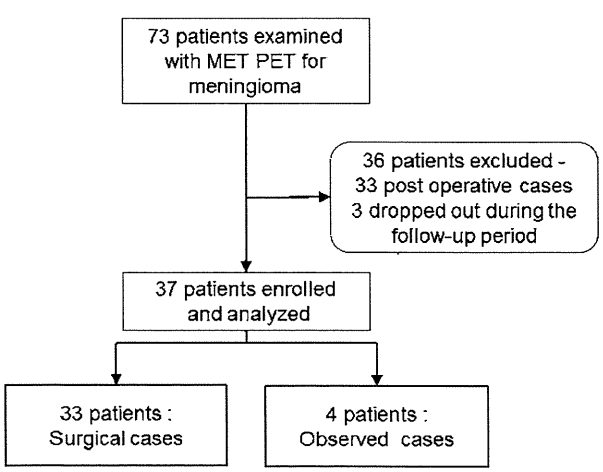

Fig. 1 Analysis of meningioma cases with MET PET

MET PET study

All patients underwent a MET PET scan with HEADTOME-IV (BGO, Shimadzu, Japan) between 1995 and 2005, Eminence-B (BGO) since 2005, and Biograph-16 (LSO, Siemens, Germany) since 2010. Twenty-six patients were examined with HEADTOME-IV. Axial and in-plane resolutions of the PET images were each 4.5 mm (in full width at half maximum), and the slice thickness was 4 mm. Twenty minutes after MET injection (4 MBq/kg), an emission scan of the brain was performed for 10 min. The emission scan was reconstructed to a matrix of 128 × 128 (using an iterative algorithm), and attenuation and scatter correction were done. The voxel size was 2 × 2 × 3.25 mm.

Ten patients were examined with Eminence-B. Axial and transaxial resolutions of the PET were each 4.5 mm (in full width at half maximum). The injection volume and timing of the scan were the same as HEADTOME-IV. The emission scan was reconstructed to a matrix of 128 × 128, and attenuation and scatter correction were done. The voxel size was 2 × 2 × 3.25 mm.

One patient was examined with Biograph-16. Axial and transaxial resolutions of the PET were 5.5 and 5.9 mm (in full width at half maximum), respectively. The injection volume and timing of the scan were the same as HEADTOME-IV. The emission scan was reconstructed to a matrix of 336 × 336, and attenuation and scatter correction were done. The voxel size was 1.02 × 1.02 × 2 mm.

All MET PET images were interpreted by an experienced neurosurgeon. The MET uptake was calculated by drawing a region of interest (ROI) using a freehand procedure. In all cases, MET uptake of the lesion was higher than in normal gray matter. In cases with a multiple meningioma, the lesion with the highest mass was evaluated. From the tumor lesion and normal reference region (frontal lobe of the normal side), the lesion to normal ratio (LN ratio) of mean MET uptake was calculated.

Surgical resection, pathological findings, and clinical follow-up

Thirty-three cases were treated with surgery, and four cases were observed. In surgical cases, GTR (Simpson grade I or II) was performed in 18 cases (55 %), and subtotal resection (Simpson grade III or IV) was performed in 13 cases (39 %). Partial resection (Simpson grade IV) was performed in one case (3 %), and a biopsy (Simpson grade V) was performed in one case (3 %). The pathological diagnosis and the WHO grade were determined by experienced

pathologists according to the WHO classification updated in 2007. The Ki-67 LI was also calculated. All patients were followed up at our out-patient clinic without any additional treatment for the tumor during the follow-up period. For the surgical cases, gadolinium (Gd)-enhanced magnetic resonance imaging (MRI) was performed every 3–6 months in the first 2 years after surgery, and then every year during the follow-up period. For the observation cases, Gd-enhanced MRI was performed more than once a year. The mean follow-up period was 80 ± 52 months (range 4–180 months). In surgical cases, the lesion was defined as a 'recurrence' when a lesion was found at the same location or a residual lesion was obviously enlarged in the radiological examinations. In non-surgical observation cases, the lesion was defined as a 'progression' when the tumor size was obviously enlarged in the radiological examinations.

We evaluated the risk factors for recurrence and progression by age, gender, location (skull base or not), extent of resection (GTR or not), Ki-67 LI, and LN ratio of MET uptake.

Statistical analysis

We evaluated the risk factors for recurrence and progression using paired *t* tests. When the data were not normally distributed, Wilcoxon's rank-sum test was used for continuous data. Fisher's exact tests were used for categorical data. Cox proportional hazards regression analysis was used for the surgical cases to assess the predictors of recurrence and progression with duration of the recurrence-free period as the time variable. A receiver operating characteristics (ROC) curve was assessed to confirm the best cutoff value of the LN ratio for recurrence and progression. All statistical analysis was performed using JMP 9 software (SAS Institute Inc.).

Results

Characteristics and pathology

During the follow-up period, six surgical patients had a recurrence, and two observation patients progressed. The characteristics of the 37 cases are shown in Table 1. Summaries of the recurrence group and the non-recurrence group are shown in Table 2. The mean age of the recurrence group was 57.9 ± 11.8 years, and that of the non-recurrence group was 53.6 ± 13.2 years. We found no significant difference in the numbers of males and females in each group.

The tumor location is shown in Table 1. We classified the tumor location into two groups: skull base and non-skull base. The recurrence rate was not significantly different between these two groups.

Two patients died during the clinical follow-up period. One (case 20) died of thyroid cancer 51 months after PET examination, and another (case 21) died due to tumor progression 4 months after PET examination. The tumors were classified by pathology as follows. Ten were meningothelial (30 %), nine were fibrous (27 %), eight were transitional (24 %), two were angiomatous (6 %), two were chordoid (6 %), one was secretory (3 %), and one was atypical (3 %). Thirty cases were WHO grade I meningiomas, and three cases were WHO grade II meningiomas. The recurrence rate was not significantly different between WHO grade I (17 %, 5/30 cases) and grade II (33 %, 1/3 cases). The mean LN ratio of WHO grade I meningiomas was 2.99 ± 1.07, and the mean LN ratio of WHO grade II meningiomas was 2.35 ± 0.36. The LN ratio was not significantly different between WHO grade I and grade II.

Extent of tumor resection and recurrence

Gross total resection was performed in 18 patients, and one patient (case 35) had a recurrence during clinical follow-up. In 15 patients, some tumor remained after the surgery. In this non-GTR group, recurrence of meningioma was observed in five patients. The recurrence rate was not significantly different between the non-GTR group and the GTR group ($p = 0.053$).

LN ratio of MET PET and Ki-67 LI for progression and recurrence

During the clinical follow-up, six cases of recurrence and two cases of progression were found. The average LN ratio of these eight cases was 3.67 ± 1.15 [95 % confidence interval (CI) 2.71–4.64] and that of the remaining 29 cases was 2.65 ± 0.86 (95 % CI 2.32–2.98). The average LN ratio of the cases with recurrence and progression was higher than that of the cases without recurrence or progression ($p < 0.01$, Fig. 2). The average Ki-67 LI of the recurrent six cases was 1.81 ± 1.21 (95 % CI 0.54–3.09), and that of the 27 cases without recurrence was 3.06 ± 3.84 (95 % CI 1.54–4.58). The Ki-67 LI was not significantly different between the recurrence group and the non-recurrence group ($p = 0.44$). No correlation was found between the LN ratio and the Ki-67 LI (Fig. 3). Risk factors evaluated with univariate analysis are summarized in Table 2. One illustrative case is shown in Fig. 4.

Table 1 Characteristics of 37 patients with meningioma

No.	Age (years)	Gender	Location	Pathological diagnosis	WHO grade	Ki-67	LN ratio	Surgery	Recurrence/ progression (months after pet exam)	Follow-up (months)
1	48	F	Parasagittal	Transitional	I	15.5	2.23	GTR	No	176
2	67	F	Parasagittal	Transitional	I	3	2.22	GTR	No	45
3	49	F	Sphenoid ridge	Chordoid	II	1.34	2.63	GTR	No	157
4	57	F	Petroclival	Secretory	I	14.4	3.00	GTR	No	40
5	49	M	Olfactory groove	Transitional	I	4.98	2.63	GTR	No	180
6	39	M	Pineal	Chordoid	II	3.03	1.95	GTR	No	26
7	61	F	Clival	Fibrous	I	4	5.10	STR	Yes (9)	141
8	43	M	Parasagittal	Fibrous	I	0.3	3.97	GTR	No	159
9	58	F	Parasagittal	Fibrous	I	1.45	3.10	GTR	No	34
10	46	F	Convexity	Fibrous	I	4.49	3.73	GTR	No	88
11	61	M	Clinoidal	Transitional	I	1.12	2.94	STR	No	152
12	79	M	Convexity	Meningothelial	I	1.26	5.38	STR	Yes (13)	56
13	57	F	Parasagittal	Angiomatous	I	2.29	3.61	STR	Yes (20)	147
14	37	F	Convexity	Meningothelial	I	2.27	3.37	GTR	No	145
15	54	F	Tentorial	Fibrous	I	0.59	3.32	STR	No	142
16	71	M	Parasagittal	Meningothelial	I	0.92	5.09	STR	No	65
17	66	F	C-P angle	Transitional	I	0.49	2.65	STR	No	138
18	22	F	Convexity	Meningothelial	I	1.3	1.98	GTR	No	130
19	60	M	Sphenoid ridge	Fibrous	I	1.33	2.90	STR	Yes (17)	71
20	74	M	Tuberculum sellae	Meningothelial	I	0.2	2.17	STR	No	51
21	39	M	Middle fossa	–	–		3.18	–	Yes (4)	4
22	75	F	C-P angle	Fibrous	I	3.5	2.35	GTR	No	54
23	52	F	Tuberculum sellae	Angiomatous	I	1	2.54	GTR	No	110
24	50	F	Sphenoid ridge	Meningothelial	I	1.26	1.65	STR	No	29
25	49	F	C-P angle	–	–	–	1.53	–	No	97
26	62	M	Convexity	Fibrous	I	3	2.86	STR	No	65
27	57	M	Convexity	Transitional	I	2.95	1.20	GTR	No	48
28	44	F	Foramen magnum	Meningothelial	I	5.6	2.64	GTR	No	48
29	48	F	Intraventricular	Fibrous	I	6.5	3.03	GTR	No	74
30	42	F	Sphenoid ridge	Transitional	I	2	2.73	STR	No	69
31	62	F	Convexity	Transitional	I	0.1	1.68	Biopsy	No	47
32	30	F	Intraventricular	–	–	–	2.49	–	No	24
33	69	F	Convexity	Meningothelial	I	0.3	1.27	GTR	No	43
34	49	M	Clivotentorial	–	–	–	2.39	–	Yes (43)	43
35	53	F	Intraventricular	Atypical	II	1.5	2.48	GTR	Yes (26)	26
36	65	M	Clival	Meningothelial	I	0.5	4.35	Partial	Yes (15)	25
37	72	M	Tentorial	Meningothelial	I	1	3.89	STR	No	23

C-P angle cerebello-pontine angle, *GTR* gross total resection, *STR* subtotal resection

In our study, the LN ratio was a significant risk factor for recurrence and progression with univariate analysis. We also evaluated risk factors using multivariate analysis. The results are summarized in Table 3. Multivariate analysis showed that the LN ratio, the extent of resection, and the WHO grade were significant risk factors for recurrence and progression. The hazard ratio of the LN ratio was 4.21. The LN ratio was the only factor examined preoperatively.

ROC curve analysis

A ROC curve was generated, and the area under the curve (AUC) was calculated to determine the best discriminating

Table 2 Evaluation of risk for recurrence and progression using univariate analysis

	Total cases		Recurrence/progression	Non-recurrence/progression	*p* value
Cases	37		8	29	
Age (years)	37		57.9 ± 11.8	53.6 ± 13.2	0.41
Gender	37	Female	3	20	
		Male	5	9	0.22
Skull base	37	Yes	5	11	
		No	3	18	0.25
LN ratio	37		3.67 ± 1.15	2.65 ± 0.86	<0.01
Extent of resection	33	GTR	1	17	
		Non-GTR	5	10	0.053
WHO grade	33	Grade I	5	25	
		Grade II	1	2	0.46
Ki-67 LI	33		1.81 ± 1.21	3.06 ± 3.84	0.44

The LN ratio was a significant risk factor for recurrence and progression

LN lesion to normal, *GTR* gross total resection, *LI* labeling index

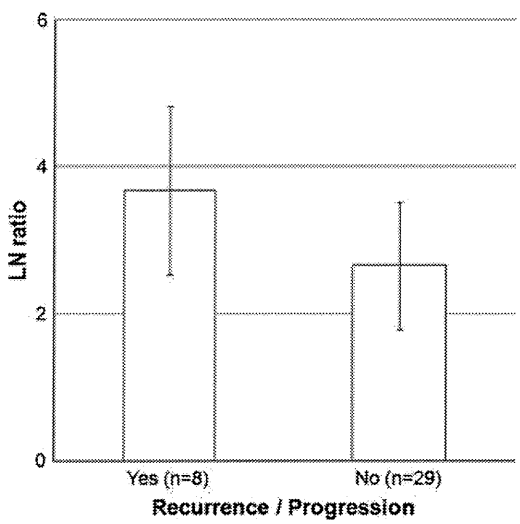

Fig. 2 LN ratio of MET PET and recurrence/progression. The LN ratio in cases with recurrence and progression was significantly higher than that in cases without recurrence and progression ($p < 0.01$)

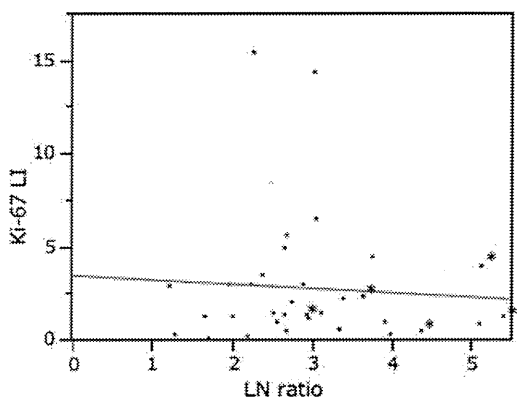

Fig. 3 Correlation between the LN ratio of MET PET and the Ki-67 LI. No correlation between the LN ratio and the Ki-67 LI was observed. *Asterisks* cases with recurrence or progression

level of the LN ratio for predicting recurrence and progression. ROC analysis confirmed 3.18 as the best predictive cutoff value of the LN ratio for recurrence and progression. The AUC was 0.754. Using the best cutoff value of 3.18, the sensitivity and specificity were 63 and 79 %, respectively (Fig. 5).

Discussion

The risk factors for recurrence and progression in meningioma have been reported in many previous studies. They include age [5, 6], gender [7], tumor size [8], calcification [7, 9], brain invasion [10], location [11], vascular density [12], Ki-67 LI [8, 13–15], extent of the resection [12, 16, 17], and WHO grade [11]. In our study, age, gender, tumor location, Ki-67 LI, and the LN ratio of MET PET were investigated. A high LN ratio was significantly correlated with tumor recurrence and progression. However, age, gender, tumor location, and KI-67 LI were not significantly correlated with tumor recurrence. These risk factors remain controversial.

Recently, the MET PET method has been used in gliomas and other intracranial tumors to evaluate the malignancy of the tumor and the proliferative activity. In previous studies of gliomas, MET uptake correlated with the WHO grade, Ki-67 LI, and patient survival [18–21]. However, the role of MET PET in meningioma is not clear. In a previous study using ^{18}F-fluorodeoxyglucose (FDG) PET, ^{18}F-FDG uptake was correlated with the Ki-67 LI but not with recurrence of the meningioma [22, 23]. Using

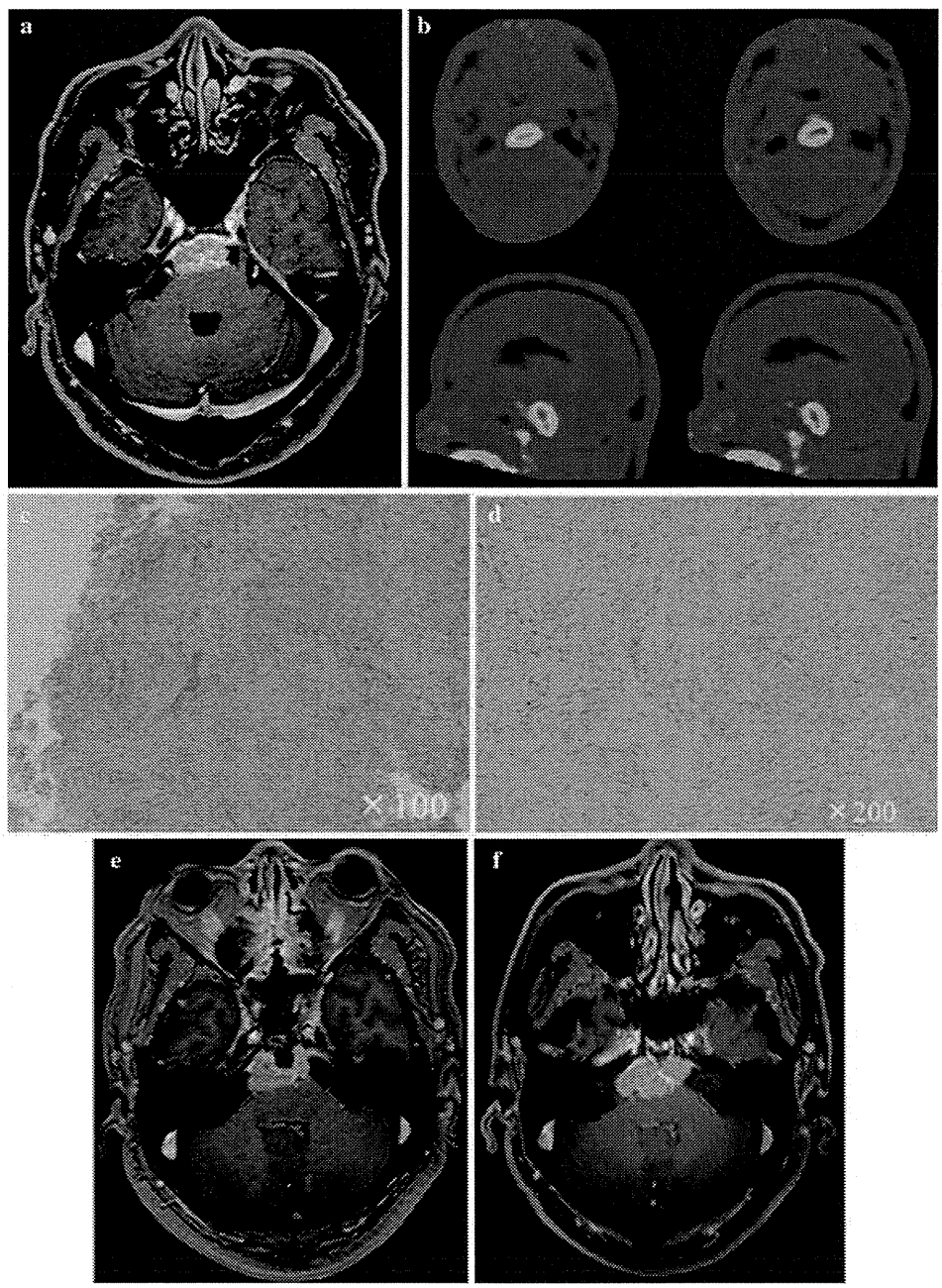

Fig. 4 Case 36. **a** Preoperative Gadolinium (Gd)-enhanced T1-weighted image. The tumor is located at the clivus. **b** ^{11}C-methionine was taken up into the tumor. The LN ratio was 4.35. **c**, **d** Photomicrograph of a sample of the lesion. Hematoxylin and eosin-stained section (**c** ×100) and Ki-67 staining (**d** ×200) of a meningioma tissue specimen. The diagnosis based on pathology was meningothelial meningioma. The Ki-67 LI was 0.5. **e** Postoperative Gd-enhanced T1-weighted image. In this case, the tumor was partially removed using a trans-sphenoidal approach. **f** Gd-enhanced T1-weighted image 15 months after surgery. The tumor had begun to grow again

kinetic analysis with ^{18}F-FDG PET, Tsuyuguchi [24] showed that the kinetic rate constant of glucose metabolism is related to the Ki-67 LI. However, that analysis requires frequent arterial blood samplings and dynamic PET scanning. The procedure is very complicated and not practical for clinical use. Moreover, the results of ^{18}F-FDG PET are influenced by blood glucose. In patients with hyperglycemia, the results may lead to overestimation [25]. Iuchi et al. [26] showed that MET uptake is significantly correlated with the count of nuclear organizer regions, which is a histological index of protein synthesis, the Ki-67 LI, and a histological index of proliferative activity. In that study,

^{18}F-FDG uptake showed no significant correlation with the Ki-67 LI or clinical malignancy. The uptake of methionine reflects amino acid transport and metabolism, but this does not mean that methionine uptake is correlated with protein synthesis and proliferation [27]. Some previous studies have shown that MET uptake correlates with microvessel density in glioma cases [28, 29], but in meningioma cases, MET uptake does not correlate with microvessel density [30]. This observation may reflect the fact that meningioma has multiple pathological subtypes and, thus, microvessel density may be different in each subtype. To evaluate the correlation between the LN ratio and microvessel density in meningioma, many cases of each subtype would be necessary.

Arita et al. [30] showed that the LN ratio of MET uptake is not significantly correlated with tumor doubling time. In this study, many asymptomatic patients were enrolled, and the mean tumor doubling time was very long (174 ± 270 months) despite a short follow-up period (26.7 ± 16.7 months). Thus, evaluation of recurrence and progression in meningioma using tumor doubling time appeared to be difficult because most meningiomas progress slowly.

Compared with ^{18}F-FDG PET, the contrast between a meningioma lesion and normal brain tissue is clear in MET PET and, thus, we can correctly define the ROI using MET PET. Recently, we have evaluated MET uptake more correctly by fusing PET images with computed tomography or MR images.

In this study, we calculated the LN ratio using the mean MET uptake of the lesion and the normal brain tissue. The methionine uptake in the tumor depends not only on the metabolic rate, but also on the vascular bed [31]. The vascular bed of the meningioma is different within the various pathological types of meningiomas [32], and the vascular bed may be variable in the same specimen. Biological activity is heterogeneous in the same meningioma lesion [33, 34]. Thus, partially high MET uptake does not always indicate a high metabolic rate of the whole tumor. In this study, we used the mean MET uptake, not the maximum MET uptake, to reduce the influence on the heterogeneity of MET uptake.

Table 3 Evaluation of risk factors for recurrence using Cox proportional hazards model

	p value	Risk ratio
Age (years)	0.28	
Gender	0.43	
Skull base	0.12	
LN ratio	0.03	4.21
Extent of resection (non-GTR/GTR)	0.014	
WHO grade (grade II/grade I)	0.0074	
Ki-67 LI	0.079	

LN ratio, extent of resection, and WHO grade were significant risk factors

LN lesion to normal, *WHO* World Health Organization, *GTR* gross total resection, *LI* labeling index

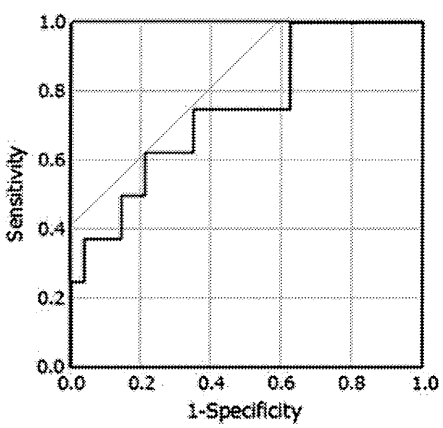

Fig. 5 ROC curve of the LN ratio. AUC of the LN ratio of MET PET was 0.754. The optimal cutoff value was 3.18. The sensitivity and specificity were 63 and 79 %, respectively

Table 4 Evaluation of risk factors for recurrence and progression excluding gross total resection cases

	Total cases		Recurrence/progression	Non-recurrence/progression	*p* value
Cases	19		7	12	
Age (years)	19		58.6 ± 12.5	57.8 ± 13.2	0.9
Gender	19	Female	2	7	
		Male	5	5	0.35
Skull base	19	Yes	5	6	
		No	2	6	0.63
LN ratio	19		3.84 ± 1.13	2.74 ± 1.02	0.04
Surgical cases			5	10	
WHO grade	15	Grade I	5	10	
		Grade II	0	0	
Ki-67 LI	15		1.87 ± 1.35	1.06 ± 0.87	0.18

Only the LN ratio was significantly different between the recurrence/progression group and the non-recurrence/progression group

LN lesion to normal, *WHO* World Health Organization, *LI* labeling index

In this study, tumor progression and recurrence were not significantly different between the GTR and non-GTR groups. However, in some cases with a high Ki-67 LI, GTR was performed, and the recurrence rate was low. GTR was a factor that strongly influenced the recurrence rate. We evaluated the recurrence and progression in the non-GTR group. The LN ratio in the group with recurrence and progression was also significantly higher than that in the group without recurrence and progression ($p < 0.05$). The Ki-67 LI was not significantly different ($p = 0.18$). Our observations are summarized in Table 4.

In our study, the LN ratio was a significant risk factor for recurrence and progression. The LN ratio of MET PET may indicate the proliferative activity of meningioma. Using ROC analysis, the AUC was 0.754, and the best cutoff value was 3.18, resulting in a sensitivity and specificity of 63 and 79 %, respectively. The sensitivity and specificity of the LN ratio were not less than those of the Ki-67 LI, as described in a previous study [35, 36].

In our study, the Ki-67 LI was not significantly different between the patients with recurrence and those without. We also found no correlation between the LN ratio and the Ki-67 LI. Some previous papers have reported that the correlation between the Ki-67 LI and tumor recurrence is controversial [4, 33, 37, 38]. Meningioma is characterized by heterogeneous biological activity within the same tumor tissue [33, 34]. It is doubtful that the Ki-67 LI obtained from a small tumor specimen can adequately evaluate the proliferative potential of the whole tumor. In fact, MET uptake is heterogeneous in a large tumor and may reflect the heterogeneity of the Ki-67 LI. The MET PET method is useful for evaluating the whole tumor. The Ki-67 LI overlaps within each grade of meningioma [39–41]. Evaluating the proliferative activity of the whole tumor and providing an accurate prognosis may be difficult with only one index.

The extent of resection was a significant risk factor as shown in a previous study [12, 16, 17]. However, the location of the tumor was not a significant risk factor in this study. Sixteen cases of skull base meningioma were included. In these cases, total resection without complications is difficult. A GTR of the tumor would reduce the risk of recurrence. This result may indicate that additional treatments are necessary for a residual tumor in which the LN ratio is higher than 3.18.

The WHO grade of meningioma was also a significant risk factor. In this study, we investigated preoperative cases and, thus, most cases were WHO grade I; only three cases were WHO grade II. Cases with WHO grade III meningioma are relatively infrequent at initial diagnosis. Almost all cases of meningioma are pathologically benign. Thus, we have to follow patients for a long time to investigate malignant changes and the prognosis. We must investigate additional consecutive cases to evaluate the largest number and the widest variety of cases.

Our study showed that the MET PET method has useful sensitivity and specificity for evaluation of recurrence and progression in meningioma. The most beneficial point is that ^{11}C-methionine PET is not invasive, whereas analysis of the Ki-67 LI requires surgery. Thus, without surgery, we can evaluate the risk of progression and recurrence and consider the treatment strategy. We can determine the risk of progression and recurrence before deciding on observation or surgery. In asymptomatic cases, high LN ratio of MET PET may be the decisive factor for determining surgical treatment. We did not evaluate a large number of cases, and thus continued collection of cases and evaluation of the data are necessary.

Conclusion

The results of our study showed that MET uptake by the meningioma was a significant prognostic factor. MET uptake was significantly higher in cases with recurrence or progression. The AUC of the LN ratio for recurrence or progression was 0.754, and the best cutoff value was 3.18. The greatest advantage associated with the MET PET method is its non-invasive nature.

Acknowledgments The authors appreciate the technical support of the radiological technologist at our institute.

Conflict of interest The authors have no personal financial or institutional interest in any of the drugs, materials, or devices described in this article.

References

1. Committee of Brain Tumor Registry of Japan. Report of Brain Tumor Registry of Japan (1984-2000) Neurol Med Chir. 2009;49 Suppl.
2. Crompton MR, Gautier-Smith PC. The prediction of recurrence in meningiomas. J Neurol Neurosurg Psychiatry. 1970;33(1): 80–7.
3. Jellinger K, Slowik F. Histological subtypes and prognostic problems in meningiomas. J Neurol. 1975;208(4):279–98.
4. Roser F, Samii M, Ostertag H, Bellinzona M. The Ki-67 proliferation antigen in meningiomas. Experience in 600 cases. Acta Neurochir. 2004;146(1):37–44 (discussion).
5. McCarthy BJ, Davis FG, Freels S, Surawicz TS, Damek DM, Grutsch J, et al. Factors associated with survival in patients with meningioma. J Neurosurg. 1998;88(5):831–9.
6. Nakamura M, Roser F, Michel J, Jacobs C, Samii M. The natural history of incidental meningiomas. Neurosurgery. 2003;53(1):62–70 (discussion-1).
7. Niiro M, Yatsushiro K, Nakamura K, Kawahara Y, Kuratsu J. Natural history of elderly patients with asymptomatic meningiomas. J Neurol Neurosurg Psychiatry. 2000;68(1):25–8.

8. Kasuya H, Kubo O, Tanaka M, Amano K, Kato K, Hori T. Clinical and radiological features related to the growth potential of meningioma. Neurosurg Rev. 2006;29(4):293–6 discussion 296-297.
9. Kuratsu J, Kochi M, Ushio Y. Incidence and clinical features of asymptomatic meningiomas. J Neurosurg. 2000;92(5):766–70.
10. Alvernia JE, Dang ND, Sindou MP. Convexity meningiomas: study of recurrence factors with special emphasis on the cleavage plane in a series of 100 consecutive patients. J Neurosurg. 2011;115(3):491–8.
11. McGovern SL, Aldape KD, Munsell MF, Mahajan A, DeMonte F, Woo SY. A comparison of World Health Organization tumor grades at recurrence in patients with non-skull base and skull base meningiomas. J Neurosurg. 2010;112(5):925–33.
12. Guevara P, Escobar-Arriaga E, Saavedra-Perez D, Martinez-Rumayor A, Flores-Estrada D, Rembao D, et al. Angiogenesis and expression of estrogen and progesterone receptors as predictive factors for recurrence of meningioma. J Neurooncol. 2010;98(3):379–84.
13. Matsuno A, Fujimaki T, Sasaki T, Nagashima T, Ide T, Asai A, et al. Clinical and histopathological analysis of proliferative potentials of recurrent and non-recurrent meningiomas. Acta Neuropathol. 1996;91(5):504–10.
14. Takeuchi H, Kubota T, Kabuto M, Kitai R, Nozaki J, Yamashita J. Prediction of recurrence in histologically benign meningiomas: proliferating cell nuclear antigen and Ki-67 immunohistochemical study. Surg Neurol. 1997;48(5):501–6.
15. Lanzafame S, Torrisi A, Barbagallo G, Emmanuele C, Alberio N, Albanese V. Correlation between histological grade, MIB-1, p53, and recurrence in 69 completely resected primary intracranial meningiomas with a 6 year mean follow-up. Pathol Res Pract. 2000;196(7):483–8.
16. Adegbite AB, Khan MI, Paine KW, Tan LK. The recurrence of intracranial meningiomas after surgical treatment. J Neurosurg. 1983;58(1):51–6.
17. Mirimanoff RO, Dosoretz DE, Linggood RM, Ojemann RG, Martuza RL. Meningioma: analysis of recurrence and progression following neurosurgical resection. J Neurosurg. 1985;62(1):18–24.
18. Ribom D, Eriksson A, Hartman M, Engler H, Nilsson A, Langstrom B, et al. Positron emission tomography (11)C-methionine and survival in patients with low-grade gliomas. Cancer. 2001;92(6):1541–9.
19. Torii K, Tsuyuguchi N, Kawabe J, Sunada I, Hara M, Shiomi S. Correlation of amino-acid uptake using methionine PET and histological classifications in various gliomas. Ann Nucl Med. 2005;19(8):677–83.
20. Kim S, Chung JK, Im SH, Jeong JM, Lee DS, Kim DG, et al. 11C-methionine PET as a prognostic marker in patients with glioma: comparison with 18F-FDG PET. Eur J Nucl Med Mol Imaging. 2005;32(1):52–9.
21. Kato T, Shinoda J, Oka N, Miwa K, Nakayama N, Yano H, et al. Analysis of 11C-methionine uptake in low-grade gliomas and correlation with proliferative activity. AJNR Am J Neuroradiol. 2008;29(10):1867–71.
22. Lee JW, Kang KW, Park SH, Lee SM, Paeng JC, Chung JK, et al. 18F-FDG PET in the assessment of tumor grade and prediction of tumor recurrence in intracranial meningioma. Eur J Nucl Med Mol Imaging. 2009;36(10):1574–82.
23. Lippitz B, Cremerius U, Mayfrank L, Bertalanffy H, Raoofi R, Weis J, et al. PET-study of intracranial meningiomas: correlation with histopathology, cellularity and proliferation rate. Acta Neurochirurgica Suppl. 1996;65:108–11.
24. Tsuyuguchi N. Kinetic analysis of glucose metabolism by FDG-PET versus proliferation index of Ki-67 in meningiomas–comparison with gliomas. Osaka City Med J. 1997;43(2):209–23.
25. Cremerius U, Bares R, Weis J, Sabri O, Mull M, Schroder JM, et al. Fasting improves discrimination of grade 1 and atypical or malignant meningioma in FDG-PET. J Nucl Med. 1997;38(1):26–30.
26. Iuchi T, Iwadate Y, Namba H, Osato K, Saeki N, Yamaura A, et al. Glucose and methionine uptake and proliferative activity in meningiomas. Neurol Res. 1999;21(7):640–4.
27. Gudjonsson O, Blomquist E, Lilja A, Ericson H, Bergstrom M, Nyberg G. Evaluation of the effect of high-energy proton irradiation treatment on meningiomas by means of 11C-L-methionine PET. Eur J Nucl Med. 2000;27(12):1793–9.
28. Okubo S, Zhen HN, Kawai N, Nishiyama Y, Haba R, Tamiya T. Correlation of L-methyl-11C-methionine (MET) uptake with L-type amino acid transporter 1 in human gliomas. J Neurooncol. 2010;99(2):217–25.
29. Kracht LW, Friese M, Herholz K, Schroeder R, Bauer B, Jacobs A, et al. Methyl-[11C]- L-methionine uptake as measured by positron emission tomography correlates to microvessel density in patients with glioma. Eur J Nucl Med Mol Imaging. 2003;30(6):868–73.
30. Arita H, Kinoshita M, Okita Y, Hirayama R, Watabe T, Ishohashi K, et al. Clinical characteristics of meningiomas assessed by ^{11}C-methionine and ^{18}F-fluorodeoxyglucose positron-emission tomography. J Neurooncol. 2012;107(2):379–86.
31. Abe Y, Matsuzawa T, Itoh M, Ishiwata K, Fujiwara T, Sato T, et al. Regional coupling of blood flow and methionine uptake in an experimental tumor assessed with autoradiography. Eur J Nucl Med. 1988;14(7–8):388–92.
32. Kimura H, Takeuchi H, Koshimoto Y, Arishima H, Uematsu H, Kawamura Y, et al. Perfusion imaging of meningioma by using continuous arterial spin-labeling: comparison with dynamic susceptibility-weighted contrast-enhanced MR images and histopathologic features. AJNR Am J Neuroradiol. 2006;27(1):85–93.
33. Siegers HP, Zuber P, Hamou MF, van Melle GD, de Tribolet N. The implications of the heterogeneous distribution of Ki-67 labelled cells in meningiomas. Br J Neurosurg. 1989;3(1):101–7.
34. Abramovich CM, Prayson RA. Histopathologic features and MIB-1 labeling indices in recurrent and nonrecurrent meningiomas. Arch Pathol Lab Med. 1999;123(9):793–800.
35. Bruna J, Brell M, Ferrer I, Gimenez-Bonafe P, Tortosa A. Ki-67 proliferative index predicts clinical outcome in patients with atypical or anaplastic meningioma. Neuropathology. 2007;27(2):114–20.
36. Kim YJ, Ketter R, Henn W, Zang KD, Steudel WI, Feiden W. Histopathologic indicators of recurrence in meningiomas: correlation with clinical and genetic parameters. Virchows Archiv. 2006;449(5):529–38.
37. Moller ML, Braendstrup O. No prediction of recurrence of meningiomas by PCNA and Ki-67 immunohistochemistry. J Neurooncol. 1997;34(3):241–6.
38. Nakaguchi H, Fujimaki T, Matsuno A, Matsuura R, Asai A, Suzuki I, et al. Postoperative residual tumor growth of meningioma can be predicted by MIB-1 immunohistochemistry. Cancer. 1999;85(10):2249–54.
39. Abramovich CM, Prayson RA. MIB-1 labeling indices in benign, aggressive, and malignant meningiomas: a study of 90 tumors. Hum Pathol. 1998;29(12):1420–7.
40. Kolles H, Niedermayer I, Schmitt C, Henn W, Feld R, Steudel WI, et al. Triple approach for diagnosis and grading of meningiomas: histology, morphometry of Ki-67/Feulgen stainings, and cytogenetics. Acta Neurochir. 1995;137(3–4):174–81.
41. Langford LA, Cooksley CS, DeMonte F. Comparison of MIB-1 (Ki-67) antigen and bromodeoxyuridine proliferation indices in meningiomas. Hum Pathol. 1996;27(4):350–4.

Journal of Clinical Neuroscience 19 (2012) 1719–1722

Contents lists available at SciVerse ScienceDirect

Journal of Clinical Neuroscience

journal homepage: www.elsevier.com/locate/jocn

Technical note

Fluorescence-guided surgery for glioblastoma multiforme using high-dose fluorescein sodium with excitation and barrier filters

Takeshi Okuda *, Hiromasa Yoshioka, Amami Kato

Department of Neurosurgery, Kinki University School of Medicine, 377-2, Ohno-Higashi, Osaka-Sayama, Osaka 589-8511, Japan

ARTICLE INFO

Article history:
Received 8 December 2011
Accepted 17 December 2011

Keywords:
Fluorescence-guided surgery
Fluorescein sodium
Glioblastoma multiforme

ABSTRACT

We have developed a technique of fluorescence-guided surgery using high-dose fluorescein sodium (20 mg/kg) with excitation and barrier filters for glioblastoma multiforme surgery. This technique was used in 10 patients, with surgery proceeding as expected in all patients. There were no complications or permanent side effects. This method uses filters to help distinguish between the usually invisible tumor and the brain surface, as well as allowing a detailed assessment of the positional relationships with tumor vessels and the surrounding normal vessels. As sufficient yellow staining was present even without filters, delicate microsurgery was also possible under a normal white-light microscope. Both environments could be used as necessary during surgery according to the requirements of resection, thereby improving the reliability and safety of surgery.

1. Introduction

In surgical resection for glioblastoma multiforme (GBM), the extent of excision has a significant effect on prognosis. Lacroix et al.[1] reported a 3.2-month longer survival for ⩾98% excision, and Stummer et al.[2] reported 4.9-month longer survival for total excision. According to these reports, ⩾98% excision is more effective than the 2.5-month longer survival offered by temozolomide,[3] which emphasizes the importance of the extent of resection. For this reason, innovative surgical approaches have been attempted with the aim of improving the resection rate. Fluorescence-guided surgery is an important surgical technique, with 5-aminolevulinic acid (5-ALA) and fluorescein sodium (FS) in use as fluorescent dyes. 5-ALA (Gliolan; Medac, Hamburg, Germany) has been reported to possess 100% tumor specificity and 85% sensitivity for GBM, and it is the most commonly used fluorescent dye for GMB surgery.[4] Many problems which need to be resolved, however, including the nature of its fluorescence, low sensitivity, and differences in fluorescence intensity. Fluorescein sodium (Alcon Japan, Tokyo, Japan) is a tracer of blood–brain barrier disruption, and enhanceable tumors are stained yellow. Although it has 0% tumor specificity, it has 100% sensitivity. Kuroiwa et al.[5] reported fluorescence-guided surgery for malignant glioma using the normal quantity of FS (8 mg/kg) with excitation and barrier filters. Subsequently, Shinoda et al.[6] reported that observation via a normal microscope under white light without using a special filter was also possible by intravenously injecting a high-dose (20 mg/kg) during GBM surgery. Shinoda et al.'s method[6] has the convenience of not using special filters, and it is now also widely used for tumors other than GBM, such as metastatic brain tumors.[7,8] We have developed a new technique of fluorescence-guided surgery for GBM surgery using high-dose FS with excitation and barrier filters and report its effectiveness.

2. Materials and methods

FS is used extensively in ophthalmology, and its safety has been established. After induction of general anesthesia and opening of the dura, high-dose FS (20 mg/kg) was injected intravenously. Tumor resection was performed >15 minutes after injection of fluorescein sodium. Excitation and barrier filters (Olympus, Shinjuku, Tokyo, Japan) were inserted into the operating microscope (OME-9000, Olympus). The excitation filter wavelength was 480 nm, and the barrier filter wavelength was 520 nm. The filters could be switched on and off easily using a microscope lever during surgery. During tumor resection, filters were first used to confirm localization of the invisible tumor in relation to the brain surface and to assess the positional relationships with the surrounding vessels – a corticotomy could then be performed with minimum invasiveness. Subsequently, most tumor resection was performed with filters off; filters were used only for locating tumor tissue, residual tumor, and the positional relationships with the surrounding vessels. All patients provided written informed consent.

* Corresponding author. Tel.: +81 72 366 0221x3547; fax: +81 72 365 6975.
E-mail address: okuda@neuro-s.med.kindai.ac.jp (T. Okuda).

0967-5868/$ - see front matter © 2012 Elsevier Ltd. All rights reserved.
http://dx.doi.org/10.1016/j.jocn.2011.12.034

Table 1
Characteristics of ten patients with glioblastoma multiforme and the results of fluorescence-guided surgery using fluorescein sodium

Patient no.	Age/sex	Location	Eloquent area	Extent of surgery	Presence of fluorescence With filter/without filter
1	61/M	FL (bilateral)	None	Biopsy (expected)	Present/Present
2	63/M	FL (bilateral)	None	Biopsy (expected)	Present/Present
3	37/M	TL (left)	Speech	Biopsy (expected)	Present/Present
4	69/M	FL (left)	Motor	SR (expected)	Present/Present
5	60/M	OL (right)	None	SR (expected)	Present/Present
6	69/M	TL(left)	Speech	GR (expected)	Present/Present
7	68/F	TL (left)	Speech	GR (expected)	Present/Present
8	79/F	FL (left)	None	GR (expected)	Present/Present
9	67/M	TL (right)	None	GR (expected)	Present/Present
10	72/F	FL (right)	None	GR (expected)	Present/Present

F = female, FL = frontal lobe, GR = gross total resection, M = male, OL = occipital lobe, SR = subtotal resection, TL = temporal lobe.

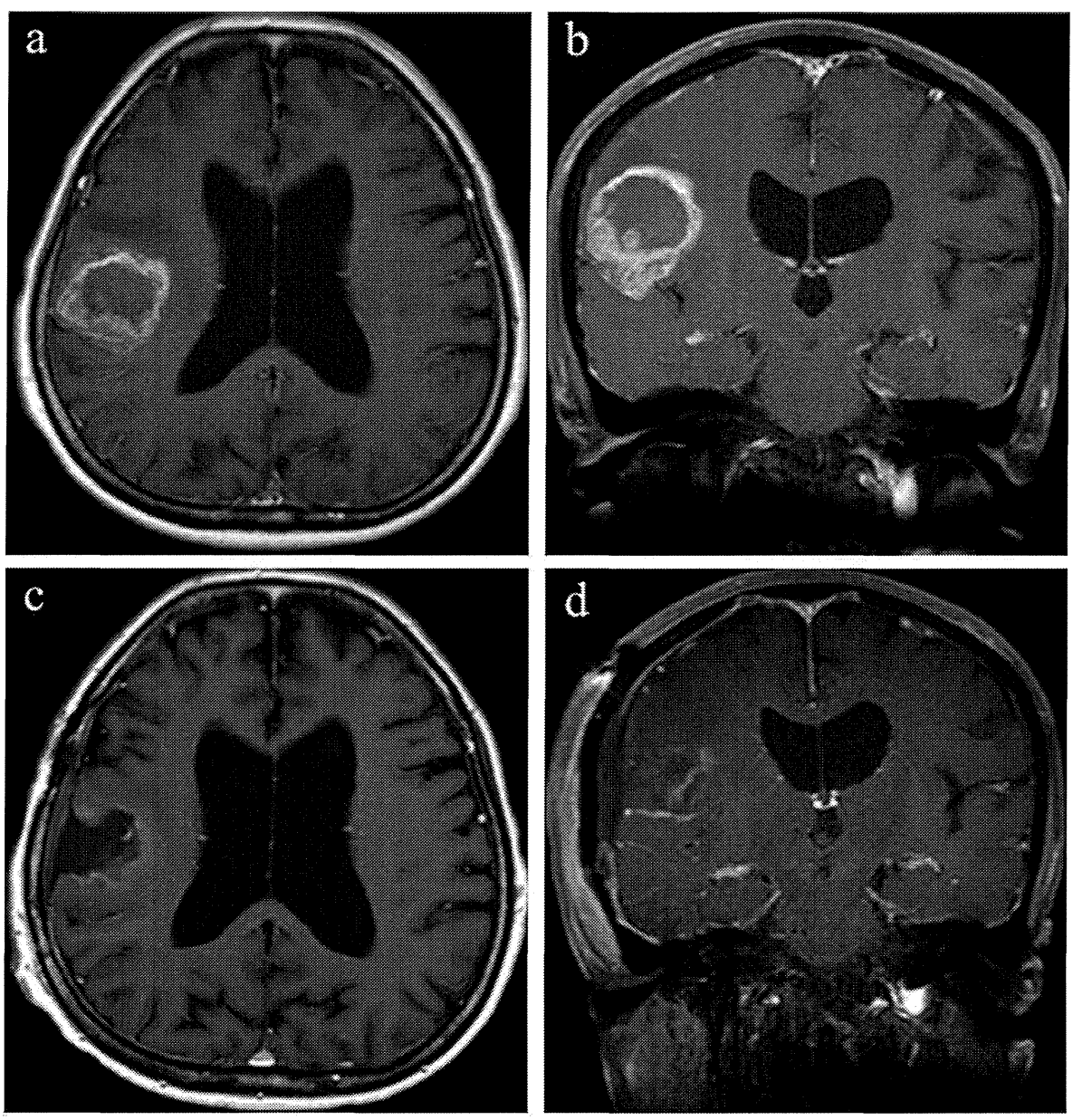

Fig. 1. Preoperative (a) axial and (b) coronal T1-weighted gadolinium-enhanced MRI showing a glioblastoma multiforme in the opercular region; and postoperative (c) axial and (d) coronal T1-weighted gadolinium-enhanced MRI showing no residual tumor and complete resection.

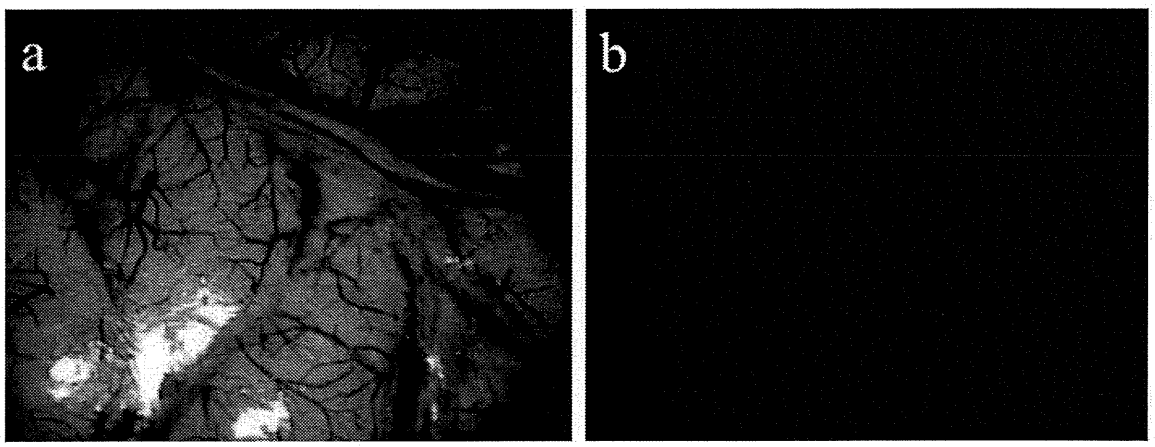

Fig. 2. Intraoperative photographs before tumor resection showing: (a) the tumor cannot be differentiated from the brain surface under a normal white-light microscope after administration of fluorescein sodium; and (b) use of excitation and barrier filters allowing visualization of the tumor below the brain surface. The Sylvian vein is also fluorescent, providing a clear view of its relationship with the tumor.

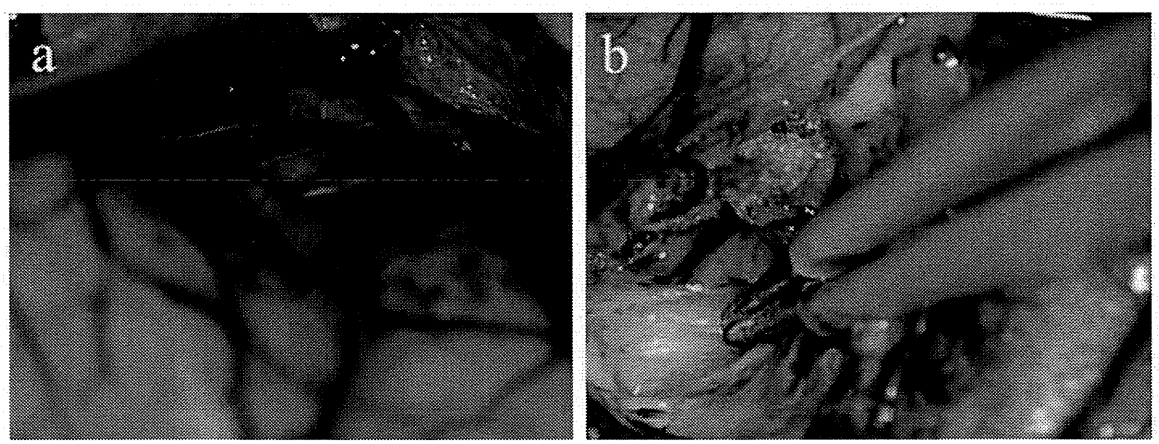

Fig. 3. Intraoperative photographs under a normal white-light microscope showing: (a) yellow staining that reveals the tumor surface in the Sylvian fissure; and (b) the boundary between the yellow-stained tumor and the surrounding brain.

3. Results

GBM surgery was performed using the injection of high-dose FS as described in all 10 patients (Table 1). Effective tumor staining and fluorescence for excision was achieved in all cases, with surgery proceeded according to the preoperative plan. Postoperatively, there was no deterioration in neurological symptoms, nor did any other complication occur. The use of FS resulted in transient yellowing of the skin, mucosa, and urine, but this spontaneously resolved within 24 hours in all patients with urinary excretion of the dye. No permanent side effects due to FS occurred.

3.1. Illustrative patient

The patient was a 72-year-old woman with a GBM in the right frontal opercular region (Fig. 1a, b). The tumor was not exposed on the brain surface, and even after FS administration, tumor localization could not be confirmed from the brain surface when the filters were off (Fig. 2a). With the filters on, however, the fluorescent tumor could be identified, and the surrounding vessels were also clearly visualized, enabling assessment of the relationship between the tumor and the cortical veins (Fig. 2b). Dissection of the tumor from normal brain tissue was performed with the filters off, since the yellow-stained tumor could be identified even under normal microscope white light (Fig. 3a, b). Gross total resection (GTR) of the tumor was performed (Fig. 4a), and the absence of residual tumor was confirmed with the filters on (Fig. 4b). Postoperative MRI also confirmed GTR (Fig. 1c, d).

4. Discussion

In general, GTR in GBM surgery is defined as total resection of the area that is contrast-enhanced on MRI.[9] Although 5-ALA has the advantage of tumor specificity, its sensitivity is not all that high, and fluorescence may appear beyond the contrast-enhanced area on the image. FS, however, has 0% tumor specificity but 100% sensitivity, and from this principle, the location of fluorescence represents only the contrast-enhanced area. Excision of areas other than the contrast-enhanced area on the image carries the risk of worsening symptoms, and for this reason, FS may be better suited as a fluorescent dye for GBM surgery than 5-ALA.

This technique combines the use of excitation and barrier filters to enable the confirmation of tumor localization from the brain surface and a detailed assessment of brain surface vasculature. This

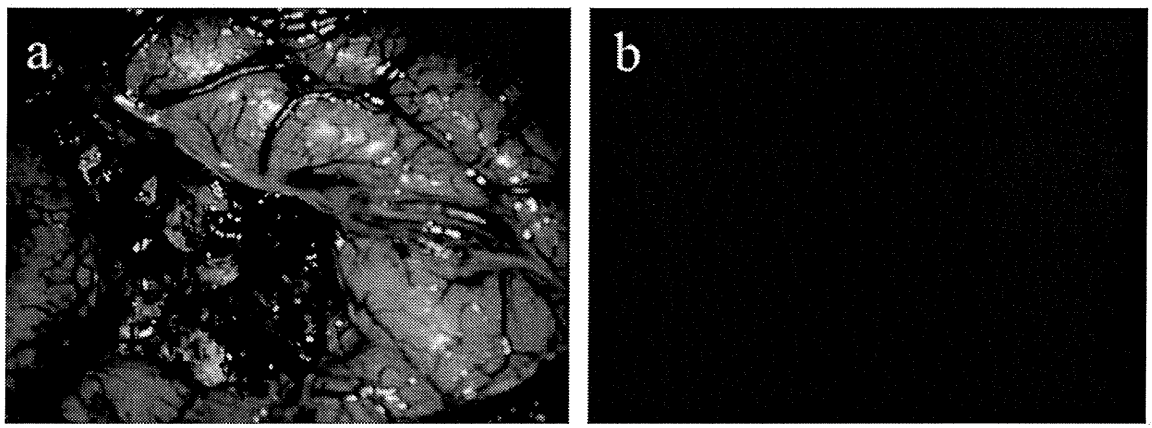

Fig. 4. Intraoperative photographs after tumor resection showing: (a) the absence of yellow-stained tissue in the resection cavity viewed under a normal white-light microscope; and (b) the absence of yellow-staining residual tumor in the resection cavity viewed with excitation and barrier filters.

Table 2
The differences between high-dose fluorescein sodium (FS) and 5-aminolevulinic acid (5-ALA)

Differences	High-dose FS	5-ALA
Route of administration	Intravenous	Oral
Tissue distribution	BBB disruption	Tumor tissue
Fluorescence area	Gd-enhanced area	>Gd-enhanced area
Color image with filter	Yellowish green	Red
Color image without filter	Yellow	Invisible
Specificity	0%	100%
Sensitivity	100%	85%
Fluorescein cerebral angiography	Very clearly	Invisible

BBB = blood–brain barrier; Gd = gadolinium.

enables corticotomy and the treatment of surrounding normal vessels to be performed with greater accuracy. This method is also used in cerebrovascular surgery, and its effectiveness in cerebral aneurysm surgery has been reported.[10] Since sufficient yellow staining can be observed under normal white-light microscopy, tumor resection can be performed while maintaining normal microscope operation. When 5-ALA is used, however, fluorescence cannot be detected without the use of filters, and surgery must be performed in a darkened room to accentuate the fluorescence, making normal microsurgery difficult. In addition, 5-ALA does not produce fluorescence of tissue other than the tumor, making assessment of the surrounding vessels difficult. Table 2 shows the differences between high-dose FS and 5-ALA during tumor resection.

Side effects of FS reportedly include anaphylactic shock brought about by 20 mg/kg of FS[11], the same dose used in our method. To date, we have used high-dose FS during brain tumor surgery in over 143 patients with malignant brain tumors, but only transient yellowing of organs such as the skin and mucosa has been observed, and no permanent or serious side effects have occurred. We therefore regard the rate of side effects due to normal drug allergy to be extremely low; however, caution is required.

5. Conclusions

Fluorescence-guided surgery using high-dose FS with excitation and barrier filters improved the reliability of resection during GBM surgery, and because it enables detailed assessment of the tumor itself, tumor vessels, and surrounding normal vessels, it was also regarded as having improved safety. Both environments, with and without filters, can be used, as necessary, according to resection requirements, making this an innovative surgical technique that can contribute to GBM surgery.

References

1. Lacroix M, Abi-Said D, Fourney DR, et al. A multivariate analysis of 416 patients with glioblastoma multiforme: prognosis, extent of resection, and survival. *J Neurosurg* 2001;**95**:190–8.
2. Stummer W, Reulen HJ, Meinel T, et al. Extent of resection and survival in glioblastoma multiforme: identification of and adjustment for bias. *Neurosurgery* 2008;**62**:564–76.
3. Stupp R, Mason WP, van den Bent MJ, et al. Radiotherapy plus concomitant and adjuvant temozolomide for glioblastoma. *N Engl J Med* 2005;**352**:987–96.
4. Stummer W, Stocker S, Wagner S, et al. Intraoperative detection of Malignant gliomas 5-aminolevulinic acid-induced porphyrin fluorescence. *Neurosurgery* 1998;**42**:518–26.
5. Kuroiwa T, Kajimoto Y, Ohta T, et al. Development of a fluorescein operative microscope for use during malignant glioma surgery: a technical note and preliminary report. *Surg Neurol* 1998;**50**:41–9.
6. Shinoda J, Yano H, Yoshimura S, et al. Fluorescence-guided resection of glioblastoma multiforme by using high-dose fluorescein sodium. *J Neurosurg* 2003;**99**:597–603.
7. Okuda T, Kataoka K, Taneda M. Metastatic brain tumor surgery using fluorescein sodium: technical note. *Minim Invasive Neurosurg* 2007;**50**:382–4.
8. Okuda T, Kataoka K, Yabuuchi T, et al. Fluorescence-guided surgery of metastatic brain tumors using fluorescein sodium. *J Clin Neurosci* 2010;**17**:118–21.
9. Pichlmeier U, Bink A, Schackert G, et al. Resection and survival in glioblastoma multiforme: an RTOG recursive partitioning analysis of ALA study patients. *Neuro Oncol* 2008;**10**:1025–34.
10. Suzuki K, Kodama N, Sasaki T, et al. Confirmation of blood flow in perforating arteries using fluorescein cerebral angiography during aneurysm surgery. *J Neurosurg* 2007;**107**:68–73.
11. Dilek O, Ihsan A, Tulay H. Anaphylactic reaction after fluorescein sodium administration during intracranial surgery. *J Clin Neurosci* 2011;**18**:430–1.

J Neurosurg 116:574–580, 2012

Slower growth of skull base meningiomas compared with non–skull base meningiomas based on volumetric and biological studies

Clinical article

Naoya Hashimoto, M.D., Ph.D.,[1] Carter S. Rabo, M.D.,[1] Yoshiko Okita, M.D., Ph.D.,[1] Manabu Kinoshita, M.D., Ph.D.,[1] Naoki Kagawa, M.D., Ph.D.,[1] Yasunori Fujimoto, M.D., Ph.D.,[1] Eiichi Morii, M.D., Ph.D.,[2] Haruhiko Kishima, M.D., Ph.D.,[1] Motohiko Maruno, M.D., Ph.D.,[3] Amami Kato, M.D., Ph.D.,[4] and Toshiki Yoshimine, M.D., Ph.D.[1]

Departments of [1]Neurosurgery and [2]Pathology, Osaka University Graduate School of Medicine, Suita; [3]Department of Neurosurgery, Osaka Prefectural Center for Adult Diseases, Osaka; and [4]Department of Neurosurgery, Kinki University School of Medicine, Sayama, Japan

Object. The precise natural history of incidentally discovered meningiomas (IDMs) remains unknown. It has been reported that for symptomatic meningiomas, tumor location can be used to predict growth. As to whether the same is true for IDMs has not been reported. This study aims to answer this question and provide biological evidence for this assumption by extending the study to involve symptomatic cases.

Methods. A total of 113 IDMs were analyzed by fine volumetry. A comparison of growth rates and patterns between skull base and non–skull base IDMs was made. Subsequently, materials obtained from 210 patients with symptomatic meningiomas who were treated in the authors' hospital during the same period were included for a biological comparison between skull base and non–skull base tumors using the MIB-1 index.

Results. The 110 patients with IDMs included 93 females and 17 males, with a mean follow-up period of 46.9 months. There were 38 skull base (34%) and 75 non–skull base (66%) meningiomas. Forty-two (37%) did not exhibit growth of more than 15% of the volume, whereas 71 (63%) showed growth. Only 15 (39.5%) of 38 skull base meningiomas showed growth, whereas 56 (74.7%) of 75 non–skull base meningiomas showed growth ($p = 0.0004$). In the 71 IDMs (15 skull base and 56 non–skull base), there was no statistical difference between the 2 groups in terms of mean age, sex, follow-up period, or initial tumor volume. However, the percentage of growth ($p = 0.002$) was significantly lower and the doubling time ($p = 0.008$) was significantly higher in the skull base than in the non–skull base tumor group. In subsequently analyzed materials from 94 skull base and 116 non–skull base symptomatic meningiomas, the mean MIB-1 index for skull base tumors was markedly low (2.09%), compared with that for non–skull base tumors (2.74%; $p = 0.013$).

Conclusions. Skull base IDMs tend not to grow, which is different from non–skull base tumors. Even when IDMs grow, the rate of growth is significantly lower than that of non–skull base tumors. The same conclusion with regard to biological behavior was confirmed in symptomatic cases based on MIB-1 index analyses. The authors' findings may impact the understanding of the natural history of IDMs, as well as strategies for management and treatment of IDMs and symptomatic meningiomas. *(DOI: 10.3171/2011.11.JNS11999)*

Key Words • **incidentally discovered meningioma** • **volumetric analysis** • **skull base** • **MIB-1 index** • **management strategy** • **oncology**

Meningiomas have increasingly been detected incidentally due to advances in neuroimaging, such as CT and MR imaging.[9] Neurological examinations and neuroradiological screening for indefinite complaints also contribute to this increase in detection, especially in advanced countries.[17] Although most IDMs can be cured surgically,[18] the morbidity and mortality associated with surgery itself cannot be determined as these tumors are generally considered asymptomatic and benign.[9] Therefore, determining the proper management for these cases is critical. However, due to the lack of knowledge regarding the exact natural history of these tumors and their potential for growth, what to consider as "appropriate" treatment remains controversial.[14]

Several authors have investigated the natural history of IDMs.[3,4,9,14,16,23,24] They have identified various factors predictive of tumor growth; however, these factors differ from study to study. Recently, we analyzed 70 IDMs using a volumetric method with a relatively long follow-up period. We concluded that most IDMs do not seem to grow for a certain period of time, and that they do not always

Abbreviation used in this paper: IDM = incidentally discovered meningioma.

grow exponentially but rather exhibit complex patterns of growth.[6] In addition, the presentation of calcification on CT or MR imaging has a negative impact on its growth.

We further surveyed other factors predictive of IDM growth, and we identified tumor location, that is, non–skull base versus skull base, as a potentially useful clinicoradiological predictor of the growth behavior of IDMs. Here, we report our results and discuss biological evidence to support these findings through expansion of the theory involving symptomatic meningiomas.

Methods

A total of 110 patients with IDMs, who are being followed up at our institution, were included in this study. The tumor growth rate of individual IDMs was analyzed using a manual volumetric method. Then, to confirm the biological differences between skull base and non–skull base tumors, 210 symptomatic patients with Grade I meningiomas, based on the WHO 2007 classification, who were treated in Osaka University Hospital, were also included. This study was approved by the ethics review board of the university.

Definition of Tumor Location

The location of the origin of the meningioma was carefully determined on MR images by N.H. and at least one of the coauthors, who are all experienced neurosurgeons (M.K., N.K., Y.F., and T.Y.). For large tumors, for which the origin is difficult to define, the most widely attached portion of the tumor in the skull was considered. In this study, we divided tumor location into 2 groups: skull base and non–skull base. Skull base origins included the olfactory groove, planum sphenoidale, cavernous sinus, sphenoid wing, clinoidal portion, tuberculum sellae, clivus, and petrous bone. Tentorial meningiomas were considered non–skull base lesions.

Volumetric Analysis of Tumor Size and Evaluation of Growth by Regression Analysis in IDMs

Between 1993 and 2009 at Osaka University Hospital, 121 patients (19 men and 102 women) were incidentally diagnosed as harboring intracranial meningiomas on the basis of MR imaging findings. We reviewed each patient's records and judged whether the tumors were totally asymptomatic or if the patient had any symptoms that could be attributed to the lesion. Meningiomas were radiologically diagnosed by the presence of an extraaxial mass, with broad-based attachment along the dura mater or with attachment to the choroid plexus in the ventricles, which were homogeneously and markedly enhanced with contrast medium as previously described.[24] Of the 121 patients, 110 who underwent MR imaging at least 3 times over the course of more than 1 year were included in this study. The results of serial MR imaging studies and clinical characteristics such as sex, age, and length of follow-up were reviewed.

Volumetric analysis and evaluation of the pattern of growth with regression analysis were conducted as previously reported.[6] Briefly, the tumor size was evaluated by volumetric assessment (volumetry) using Scion Image for Windows software (Scion Corp.). The enhanced area of the tumor in each slice image was measured by manual tracing of the tumor boundaries, and then the sum of the enhanced areas was multiplied by the slice interval of the MR imaging series. The absolute growth rate (cm^3/year) and relative growth rate (%/year) were calculated for each tumor, according to the equation described elsewhere.[14] The percentage of growth (growth volume/initial tumor volume) was calculated as well.

Inaccuracy of measurement from 2 sources of errors (one caused by using an MR imaging series with thick slice intervals and the other by manual tracing of the tumor) were addressed. For the former, we described a preliminary study with 10 cases and showed that volumetry with an MR imaging series using 6.0-mm slice intervals was estimated to show acceptable accuracy for evaluating tumor volume, compared with an MR imaging series using 2.0-mm slice intervals in the same patients.[6] This preliminary study revealed that a change in tumor volume (a percentage of growth or reduction in volume) less than 15% can be thought of as representing a measurement error. To offset the second source of measurement error, we evaluated 70 IDMs and measured them 3 times. We found that the obtained values 2 standard deviations from the calculated measurements corresponded to a change of less than 15% in each tumor volume. Considering the results from these validation studies, the cutoff for tumor growth or reduction in volume was set to 15% in this study.

The time-volume curves were plotted for each tumor, and regression analysis was performed for the group with growth. Growth curves were fitted to both exponential growth and linear growth as previously reported.[6] Regression coefficients were calculated for each regression analysis and examined statistically for significance. If the growth curve fit both exponential and linear curves statistically, the tumor was categorized according to the curve with the larger coefficient of determination (R^2). In each case in which the pattern of growth fit either exponential or linear growth, tumor doubling time was estimated from each regression equation.

Biological Differences Between Skull Base and Non–Skull Base Meningiomas

To evaluate biological differences between skull base and non–skull base meningiomas, we subsequently analyzed 210 consecutive meningioma specimens, which were surgically obtained during the same period (1993–2005). All meningiomas were histologically defined as Grade I tumors based on the WHO 2007 classification. Atypical (Grade II) and anaplastic (Grade III) tumors were excluded. Magnetic resonance imaging studies used to determine tumor location and clinicopathological characteristics such as sex, age, and histological subtype were reviewed. The MIB-1 indices were also obtained for all 210 specimens as previously described.[13]

Statistical Analysis

Regression analysis and other types of statistical analysis such as the Fisher exact test and Mann-Whitney U-test for independence were performed using statistical

software (version 5.0, Statview, SAS Institute, Inc.) with a p value < 0.05 considered significant.

Results

Volumetric Comparison of Growth Rates and Patterns Between Skull Base and Non–Skull Base Meningiomas

Demographic data are summarized in Table 1. A total of 113 IDMs from 110 patients were included in this study; 2 patients had multiple tumors. There were 93 women and 17 men, and the mean age was 66.8 years (range 37–91 years). The mean follow-up period for sequential MR images was 46.9 months, ranging from 12 to 121 months. Table 2 shows the distribution of the cases based on location. Thirty-eight (34%) were located in the skull base and 75 (66%) were not.

Of the 113 IDMs, 42 tumors (37%) showed no growth during the follow-up period and 71 (63%) showed growth. Interestingly, when all IDMs were divided into skull base and non–skull base categories, only 15 (39.5%) of 38 skull base meningiomas showed growth, whereas 56 (74.7%) of 75 non–skull base meningiomas showed growth (Fig. 1; $p = 0.0004$, Fisher exact test). Of the 38 skull base IDMs, 22 (57.9%) did not grow, and 1 reduced in volume.

As shown in Table 3, of the 71 IDMs that showed growth, no statistically significant difference was noted between the skull base and non–skull base groups in terms of mean age, sex, follow-up period, or initial tumor volume. However, the annual relative growth rate ($p = 0.009$) and the percentage of growth ($p = 0.002$) were much lower in the skull base group than in the non–skull base group. Accordingly, with slower growth rate, the tumor doubling time ($p = 0.008$) was much higher in the skull base group.

To further exemplify the differential growth rate between the 2 groups, the case of a 67-year-old man with multiple meningiomas, who underwent follow-up for 25 months, is presented. The patient had 1 cavernous and 2 convexity meningiomas (Fig. 2). The doubling time for the skull base tumor was 261 months, whereas for the 2 convexity-located tumors, it was 162 and 116 months, with the latter showing growth of more than 15%.

We also analyzed the growth pattern of these tumors (Table 4). Unexpectedly, 60% of skull base IDMs showed an exponential pattern of growth, whereas 32% of non–skull base IDMs showed an exponential pattern. Only 14% of non–skull base tumors showed no trend in growth pattern. In Fig. 2 (dotted lines), we can see that the cavernous tumor fitted better to an exponential curve and the 2 convexity tumors fitted better to a linear pattern using regression analysis. However, it is important to note that the R^2 for the 3 tumors statistically fit both linear and exponential curves (Fig. 2B). But as described in the methodology, in situations like this, the tumor will be categorized based on the pattern with a larger R^2.

The number of patients who became symptomatic and underwent treatment during the follow-up period was also different between the 2 groups (Table 5). Only 1 (2.6%) of 38 patients with skull base IDMs underwent surgery, whereas 6 (8.0%) of 75 patients with non–skull base IDMs needed surgery or radiotherapy.

Biological Differences in Skull Base and Non–Skull Base Meningiomas

To clarify the biological meaning of the volumetric results, we went back to the surgical cases seen in the same period. A summary of demographic data for the 210 consecutive symptomatic meningiomas is shown in Table 6. The mean age was 57.2 years (range 16–90 years). The incidence of male sex (25.7%) seemed higher in this series than in that of the IDMs, but it is comparable to the previously reported incidence.[18] Histological subtypes were also verified and consisted of meningothelial (44.3%), transitional (21.0%), fibrous (19.0%), angiomatous (5.2%), psammomatous (5.2%), and other (5.2%) subtypes. There were 94 skull base and 116 non–skull base meningiomas. No statistical difference was noted according to the age or sex ratio. However, the mean MIB-1 index for skull base tumors was markedly low (2.09%) compared with that for non–skull base tumors (2.74%; $p = 0.013$; Table 6 and Fig. 3).

Because male sex is a well-known factor that affects the biological behavior of meningiomas in general, the difference between female and male sex was also analyzed. As expected, the highest mean MIB-1 index (3.16%) was seen in males with non–skull base tumors, and the lowest (1.82%) in females with skull base tumors. A statistically significant difference was observed between all male and all female cohorts ($p = 0.045$), as well as between male and female cohorts with skull base tumors ($p = 0.021$; Table 7).

Discussion

Several reports have been published regarding the

TABLE 1: Demographic data of 113 IDMs for volumetric analyses

Variable	All	Skull Base	Non–Skull Base
no. of cases (%)	113	38 (34)	75 (66)
mean age in yrs (range)	66.8 (37–91)	66.8 (40–84)	66.8 (37–91)
sex ratio (F:M)	93:17	29:9	64:8
mean follow-up period in mos (range)	46.9 (12–121)	40.3 (12–100)	50.3 (12–121)
mean initial tumor volume in cm^3 (range)	9.79 (0.32–86.62)	12.22 (0.56–86.62)	8.56 (0.32–74.69)
no. w/o growth (%)	42 (37)		
no. w/ growth (%)	71 (63)		

TABLE 2: Distribution of all IDM cases based on location

Location	No. of Cases
convexity	35
falx	17
petroclival	17
parasagittal	14
sphenoid wing	7
cavernous	6
intraventricular	4
planum sphenoidale	4
tentorium	4
olfactory	3
other	2

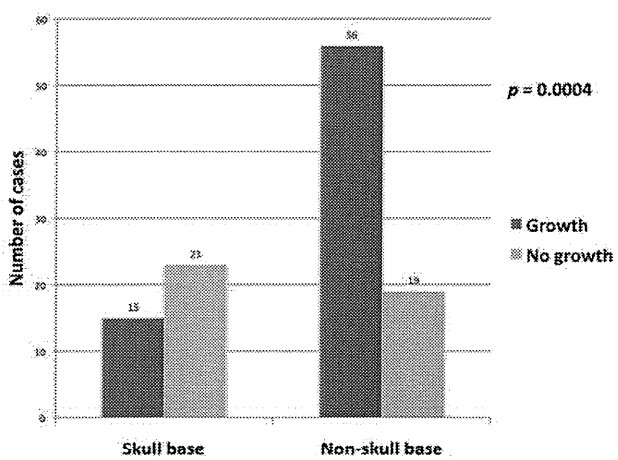

FIG. 1. Incidence of meningiomas showing growth and no growth in skull base and non–skull base tumors. Fifteen (39.5%) of 38 skull base tumors showed growth, whereas 56 (74.7%) of 75 non–skull base tumors showed growth ($p = 0.0004$, Fisher exact test).

natural history of IDMs using various means of growth measurement, some using linear (diameter)[4,9,16,21,23] and some using volumetric[6,14,15,24] methods. According to these studies, the natural history of IDMs can be summarized in 3 points. First, most IDMs (or at least a subset of IDMs) may not grow for a certain period of time. Second, for tumors that grow, the rate of growth seems slow. In our previous report, the mean tumor volume doubling time in growing IDMs was 93.6 months (7.8 years). Finally, hyperintensity on T2-weighted imaging is positively correlated with growth, whereas the presence of calcification is negatively correlated with tumor growth. As to the impact of tumor location on growth behavior, probably because of the small number of patients, this has yet to be reported. In this paper, we found that IDMs in the skull base tended not to grow when compared with those in non–skull base locations. Furthermore, even if these tumors grow, the rate of growth was significantly lower in terms of the percentage growth, annual growth rate, and rates of experiencing symptoms and undergoing treatment.

In this report, we also found that there was a statistically significant difference in the MIB-1 index, which is thought of as a biological marker of cell proliferation, between skull base and non–skull base meningiomas. This is in line with previous studies indicating the existence of biological differences between the two.[8,10,11,20] Kasuya et al.[8] reported that male sex, the absence of calcification on imaging, and non–skull base location are independent risk factors for a high MIB-1 index by logistic regression analysis among 342 consecutive surgical cases. More recently, McGovern et al.[11] made an important note that meningiomas with a non–skull base location are more likely to have a higher MIB-1 index and recur with a higher grade than those within the skull base. Sade et al.[20] found that the incidence of Grade II and III tumors is significantly higher outside the skull base (12.1%) than in the skull base (3.5%) from the records of 794 consecutive patients. Mahmood and colleagues[10] likewise noted that among their 319 patients, 25 had Grade II and III tumors, of which, 7 (28%) were located at the skull base and 18 (72%) were outside the skull base. In the latest study from

TABLE 3: Comparison between skull base and non–skull base lesions in 71 growing IDMs*

Variable	Skull Base (range)	Non–Skull Base (range)	p Value	Statistics Used
no. of cases	15	56		
mean age in yrs	69.5 (40–83)	66.6 (37–91)	0.320	M-W
sex ratio (F:M)	11:4	48:6	0.207	Fisher
mean follow-up period in mos	49.3 (20–100)	53.1 (12–121)	0.485	M-W
mean initial tumor volume in cm^3	14.71 (0.79–86.62)	8.11 (0.32–74.69)	0.163	M-W
absolute growth rate in cm^3/yr	1.20 (0.02–7.85)	1.15 (0.04–11.33)	0.662	M-W
relative growth rate %/yr	6.84 (2–24)	13.78 (2–74)	0.009†	M-W
% growth	25.56 (15.57–43.27)	94.83 (16.11–1519.67)	0.002†	M-W
mean tumor doubling time	160.8 (39–383)	111.5 (15–420)	0.008†	M-W

* M-W = Mann-Whitney.
† Statistically significant.